

A Neural Non-linear Predictive Control for PEM-FC

This paper deals with the application of non-linear predictive control with neural networks to Proton Exchange Membrane Fuel Cells (PEM-FC). The control objective is to regulate the cell voltage, acting on the hydrogen pressure, trying to reduce the variation of the input control variable. An analysis of the non-linearities of the fuel cell stack has been carried out, making use of a suitable fuel cell model. The non-linear predictive control has been implemented by several neural networks (multi value perceptrons), after dividing the operating domain into three areas according to the cell current value (low loads, quasi-linear zone and high loads). Simulation results have been provided and discussed, showing the goodness of the proposed non-linear control technique in reducing the variations of hydrogen pressure.

Keywords: PEM-FC, Non-linear Control, Predictive Control, Neural Networks.

1. INTRODUCTION

Over the last few years the fuel cells have been actively studied for their promising capability for alternative stationary and mobile power generation. Fuel cells in general show 1) good efficiency, even at reduced loads, which is generally required in ground vehicle propulsion, in comparison with heat engines, 2) low audible emissions, 3) low emissions of pollutants, 4) reliability and durability. In particular Proton Exchange Membrane Fuel Cells (PEM-FC) seem to be a good alternative for distributed generation (DG) [1] and ground vehicle applications, because of high power density, solid electrolyte, low corrosion, low-temperature operation. However, some issues are still of concern, in particular their cost, their size and weight, and the complexity of peripheral devices. Moreover there are some problems related to the dynamic response [1][2], especially in terms of fast load change response, peak power and peak current capability.

Since fuel cells generation systems have low voltage and high current output characteristic, the system performance is very sensitive to load variations [3], which means that any control system should compensate this by making the output voltage as constant as possible while penalizing variations in the gas pressure input control variable, which is beneficial for improving the life of the

Corresponding author : Marcello.pucci@ieee.org
ISSIA-CNR (Institute on Intelligent Systems for the
Automation), Section of Palermo, viale delle scienze snc,
90128 Palermo, Italy.

Copyright © JES 2005 on-line : www.joes.org.uk

stack as well as for reducing the maintenance costs of the fuel cell generation system [4].

However, since the fuel cell is an electrochemical device and has nonlinear characteristics, it is very difficult to control it, and this control task is even more difficult when all the fuel cell generation plant is considered, which consists also of many nonlinear subsystems interacting with others [5]. Many dynamical fuel cell system models have been proposed so far. In [6] a simplified model has been developed in which both the reformer and the stack have been approximated by first-order systems and a fuzzy control has been designed for improving the system performance. In [4] a control oriented model has been developed, which is an improvement of a former model [7][8], capable of predicting the output voltage of the PEM-FC as a function of the actual current load also taking into account its dynamical behaviour in a way which makes it suitable for electrical engineering purposes. This has made it possible to test a neural optimal control (NOC) for achieving reduced pressure variations [9]. This model has proved particularly interesting to test different control techniques for PEM-FC.

This paper makes use of this model in order to test a neural non-linear predictive control strategy [10] so as to obtain the same above control objectives. At first, a analysis of the non-linearities of the fuel cell stack has been made, making use of the above FC model. In particular, this analysis has been carried out by projecting the 4-dimension (hydrogen pressure, current, voltage and temperature of the cell) data of the model into a 2-dimensional and 1-dimensional space. Then the non-linear predictive control has been implemented by several neural networks (multi value perceptrons), after dividing the operating domain into three areas according to the cell current value (low loads, quasi-linear zone and high loads). Simulation results have been provided, showing the goodness of the proposed non-linear control technique in reducing the variations of hydrogen pressure.

2. DYNAMIC MODEL OF THE PEM-FC

Today, there are many different technologies associated with Fuel Cell based energy conversion. The specific technology to be used depends mainly on the amount of energy required by the specific application. For low-power domestic appliances, the most used technology is currently the PEM-FC.

The PEM-FC converts chemical energy into electric one, by employing hydrogen (H_2) as fuel and oxygen (O_2) as oxidizer, giving heat and water as undesired products. A typical generation scheme based on a PEM-FC is shown in Fig. 1.

In literature, different mathematical models have been devised to simulate the behaviour of a PEM-FC. Some are based on curve-fitting experiments [11], others are semi-empirical models that combine experimental data with parametric equations adjusted by comparison with cells physical variables like pressure and temperature [12]. In both cases, the concentration over-potential phenomenon, which is crucial in describing the dynamical behaviour of such systems, is not adequately modelled. The work developed in [4][9] correctly considers this effect, and for this reason has been adopted as a benchmark for the simulations described in the following.

The output voltage V_{FC} of a single cell can be written as:

$$V_{FC} = E_{Nernst} - V_{act} - V_{ohmic} - V_{con} \quad (1)$$

where E_{Nernst} is the thermodynamic potential of the cell, which represents the reversible voltage; V_{act} is the activation overpotential, caused by the activation of the anode and the cathode (a measure of the voltage drop of the electrodes); V_{ohmic} is the ohmic overpotential which takes into account the resistances during conduction of the protons through the solid electrolyte and the electrons through their path; V_{con} is the concentration overpotential, which considers the voltage drop caused by the reduction of concentration of reactants gases or, alternatively, by the transport of masses of oxygen and hydrogen. As clearly written in [4] there is another voltage drop term associated with the internal currents, which is the fuel crossover [12]. This effect has been considered in the adopted model, considering a constant current density even at no-load. In synthesis, E_{Nernst} represent the no-load voltage, while the sum of all the other terms gives the reduction of the useful voltage V_{FC} achievable at the cell terminals, when a certain load current is required.

For n cells connected in series, forming a stack, the voltage V_s is calculated as

$$V_s = n V_{FC} \quad (2)$$

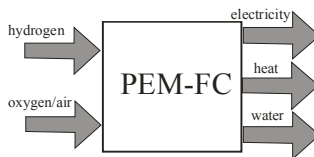


Fig. 1: Input/output representation of a PEM-FC

2.1 Cell Reversible Voltage

The reversible voltage of the cell (E_{Nernst}) is the open-circuit voltage and is computed from a modified version of Nernst equations, considering the possible variations of temperature from the standard value of 25 °C.

$$E_{Nernst} = 1.229 - 0.85 \cdot 10^{-3} (T - 298.15) + 4.31 \cdot 10^{-5} T \left[\ln(P_{H_2}) + \frac{1}{2} \ln(P_{O_2}) \right] \quad (3)$$

where T is the cell operation temperature in [K], P_{H_2} and P_{O_2} are respectively the hydrogen and oxygen partial pressures in [atm].

2.2 Activation Overpotential

The activation overpotential, including both the anode and the cathode, can be computed as:

$$V_{act} = - \left[\xi_1 + \xi_2 T + \xi_3 T \ln(c_{O_2}) + \xi_4 T \ln(i_{FC}) \right] \quad (4)$$

where i_{FC} is the cell load current in [A], and ξ 's are the parametric coefficients, defined on the basis of kinetic, thermodynamic and electrochemical phenomena [7][8]. C_{O_2} is the concentration of oxygen in the catalytic interface of the cathode in [mol/cm³], computed on the basis of the oxygen partial pressure and cell temperature as:

$$c_{O_2} = \frac{P_{O_2}}{5.08 \cdot 10^6 e^{-\left(\frac{498}{T}\right)}} \quad (5)$$

2.3 Ohmic Voltage drop

The ohmic drop is caused by the electrons transfer through the collecting plates and the carbon electrodes, and by the protons transfer through the solid membrane. It is computed as:

$$V_{ohmic} = i_{FC} (R_M + R_C) \quad (6)$$

where R_C represents the resistance to the transfer of protons through the membrane, usually considered constant. R_M is the equivalent resistance of the membrane, calculated as:

$$R_M = \frac{\rho_M \ell}{A} \quad (7)$$

where ρ_M is the specific resistivity of the membrane for the electron flow in [Ω cm], A is the cell active area in [cm²] and ℓ is the thickness of the membrane in [cm].

Since the adopted membrane is of the Nafion type, the following expression of the resistivity of the membrane has been used [7][8]:

$$\rho_M = \frac{181.6 \left[1 + 0.03 \left(\frac{i_{FC}}{A} \right) + 0.062 \left(\frac{T}{303} \right)^2 \left(\frac{i_{FC}}{A} \right)^{2.5} \right]}{\left[\psi - 0.634 - 3 \left(\frac{i_{FC}}{A} \right) \right] \exp \left[4.18 \left(\frac{T-303}{T} \right) \right]} \quad (8)$$

where the exponential term in the denominator takes into consideration temperature deviation from 30°C and ψ is an adjustable parameter, depending on the relative humidity and stoichiometric relation of the anode gas, which assumes a maximum value of 23.

2.4 Concentration Overpotential

The mass transport modifies the concentration both of oxygen and hydrogen, which causes the reduction of the partial pressures of the gases. The reduction of the partial pressures of gases depends on the load current and the characteristics of the cell. To define this voltage drop term, a maximum current density J_{\max} is defined, with which the cell works at the same rate of the maximum supply speed. On this basis, the concentration overpotential can be computed as:

$$V_{con} = -B \ln \left(1 - \frac{J}{J_{\max}} \right) \quad (9)$$

where B is a parametric coefficient, which depends on the cell, and J represents the actual current density of the cell in $[A/cm^2]$.

2.5 Dynamics of the Cell

The dynamics of the cell is mainly governed by the so called “*charge double layer*” effect. When two differently charged materials are kept in contact, either a charge accumulation on their surfaces or a load transfer from one to another occur. The charge layer in correspondence of the electrolyte/electrode interface behaves as a storage of electrical charges, and therefore, from the electric circuit point of view, can be represented by a capacitor. At each voltage variation, a time is required for charging, in case of voltage increase, or vanishing, in case of voltage decrease. This time delay affects the activation and concentration overpotential, and not the ohmic drop, whose variation can be, however, considered instantaneous.

The activation and concentration overpotentials can be modelled as first-order delay elements with a time constant $\tau = C R_a$, where C is the equivalent capacitance in [F] and R_a is the equivalent resistance in [Ω].

$$\frac{d(v_{act} + v_{con})}{dt} = \frac{1}{C} i_{FC} - \frac{1}{\tau} (v_{act} + v_{con}) \quad (10)$$

The time constant τ governing the dynamics is variable with the load conditions, since the equivalent resistance R_a is a function of the activation and concentration overpotentials and load current:

$$\tau = CR_a = C \left(\frac{V_{act} + V_{con}}{i_{FC}} \right) \quad (11)$$

3. VALIDATION OF THE MODEL

As recalled above, the dynamic model proposed in [4] has been employed for the simulations. A single PEM-FC model Ballard Mark V with a membrane model Nafion 117, fed by gases O_2 and H_2 , has been simulated to validate the model. Tab. I shows all the parameters used to model the cell.

Tab I: Parameters of the Ballard Mark V Fuel Cell

Parameters	Value	Parameters	Value
T	343 [K]	ξ_1	-0.948
A	50.6 [cm ²]	ξ_2	0.00286+0.0002 ln(A)+(4.3 10 ⁻⁵) ln(C _{H2})
P _{H2}	1 [atm]	ξ_3	7.6 10 ⁻⁵
P _{O2}	1 [atm]	ξ_4	-1.93 10 ⁻⁴
B	0.016 [V]	ψ	23
R _C	0.0003 [Ω]	J _{max}	1.5 A/cm ²
l	178 [μm]	J _n	1.2 A/cm ²

The cell polarization curve gives the fuel cell output voltage as a function of the current density in steady-state. Fig. 2 shows the results obtained with the proposed model [4] in comparison with those obtained experimentally [7][8]. It can be observed a very good agreement of the simulated curve with the experimental one, with a percent error in the quasi-linear zone of the characteristics lower than 3%. Fig. 3 shows the family of control characteristics of the Ballard Mark V, which give the voltage of the cell versus the hydrogen partial pressure, given a constant load current of the cell. As the stoichiometric consumption rate for the two gases is constant, the oxygen partial pressure is considered in these curves half of the hydrogen partial pressure. Therefore in the control systems explained in the following, only one controller has been adopted in conjunction with two independent gains, one for hydrogen line

actuator and the other for the oxygen line actuator. These curves have been plotted at three values of load current for each of the three zones of the polarization curve (low loads, quasi-linear zone, and high loads). They show that, the higher the load current, the higher the hydrogen pressure needed to obtain a given value of the cell voltage. Moreover, at 75 A load, in nonlinear zone, even with the maximum allowed value of hydrogen pressure of 10 atm, the maximum achievable voltage for each cell is only about 0.35 V.

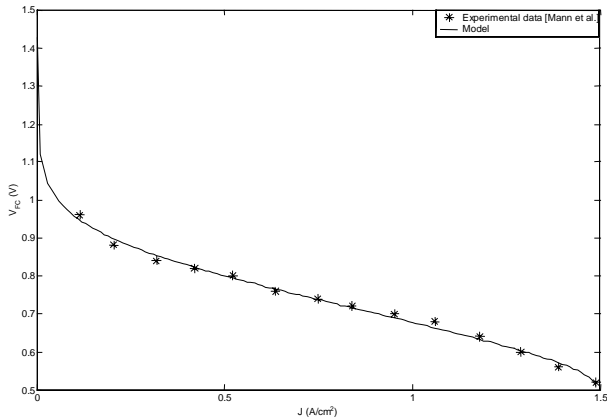


Fig. 2: Ballard Mark V polarization curve

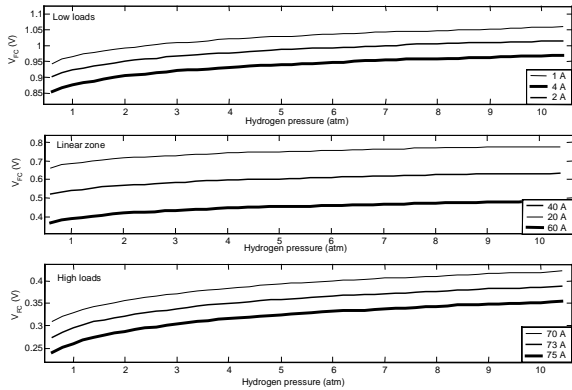


Fig. 3: Control characteristics of the Ballard Mark V in the 3 working zones

The dynamic behaviour of a cell stack of 32 series connected Ballard Mark V has been simulated in Matlab[®]-Simulink[®] environment. The capacitor C has been given the value of 3 [F] [4]. The cell has been fed with a 4 atm hydrogen partial pressure and 2 atm oxygen partial pressure at the working temperature of 10°C. Starting from a load current of 5 A, a step load insertion of 50 A followed by its step rejection has been given. Fig. 4 shows the obtained

waveforms of the cell stack voltage, power and load current. These figures clearly show that, when the load is inserted, a reduction of the voltage occurs with an increase of the generated power which exhibits, as confirmed in [1][4], an overshoot during the ascending transient.

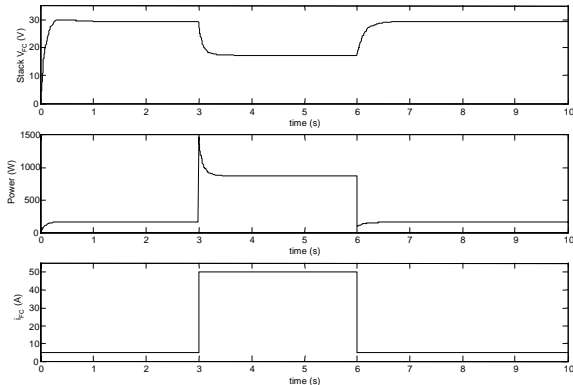


Fig. 4: Voltage, power and load current of a fuel cell stack during load insertions and successive reduction

4. NON-LINEARITY ANALYSIS OF POLARIZATION MANIFOLD

Here the polarization manifold is defined as the hypersurface in the four-dimensional space given by voltage, current, H_2 pressure and temperature. Tests of nonlinearities are presented in order to determine the best possible control design. To this aim, the neural network called Curvilinear Component Analysis (CCA, [13]) has been used. It is a self-organizing neural network which captures the data manifold in the original space and projects it in a nonlinear way into a lower-dimensional space, e.g for visualization purposes. This projection tries to respect the data interdistances: if two points in the original space are distant of a quantity \mathbf{dy} , their projections are distant of a corresponding quantity \mathbf{dx} , in such a way to be as closest as possible to \mathbf{dy} . If all possible interdistances \mathbf{dy} , \mathbf{dx} are represented in a diagram $\mathbf{dy-dx}$, it is obvious that, if the original manifold is linear, all points lie on the bisector. If not, the points bend below it. In this sense, this diagram can be considered as a nonlinearity test. If the polarization manifold is projected to the two-dimensional space, data are represented by three straight lines (see Fig.5).

These lines mean that the polarization manifold is inherently unidimensional, in the sense that it is nearly piecewise linear: the three lines correspond to different ranges of current, i.e. low currents (less than 4 A), intermediate currents (between 5 A and 69 A) and high currents (more than 71.5 A). If the

polarization manifold is considered only for currents between 4 A and 5 A (first knee in Fig.2), non-linearities appear, as can be seen in Fig.6 and 7.

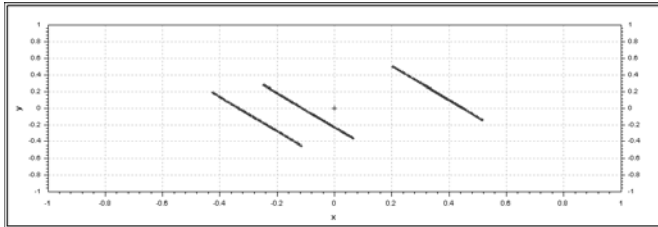


Fig.5 : CCA two-dimensional projection of the polarization manifold

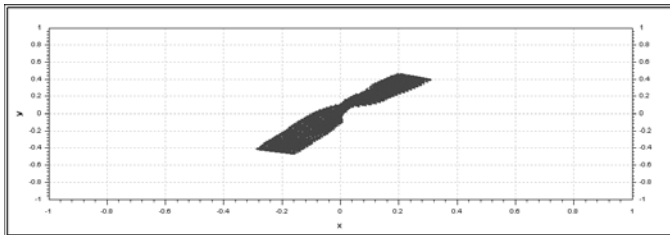


Fig.6: CCA two-dimensional projection of the polarization manifold for the first knee

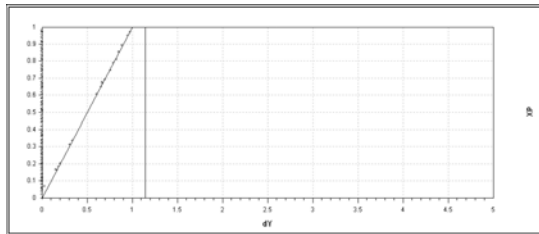


Fig.7 : Diagram $dy-dx$ of the CCA two-dimensional projection for the first knee.

Fig.6 shows the first knee in two-dimension and is caused, in a first approximation, by the transition from the unidimensional space for low currents into the one for intermediate currents. The corresponding diagram $dy-dx$ (see Fig.7), shows two clusters: the first is around the bisector (the quasi-linear manifold for intermediate currents), the second on the y-axis, because CCA here is able only to unfold one unidimensional manifold. The same considerations can be repeated for the transition from the range of intermediate currents into the range of high currents (second knee).

As a consequence of the above analysis, the polarization manifold is therefore projected into the 1-dimensional space. Fig. 8 shows the corresponding diagram $dy-dx$. Here the nonlinearities are more apparent: the two knees are represented by the two clusters on the left of the bisector and by the bending data.

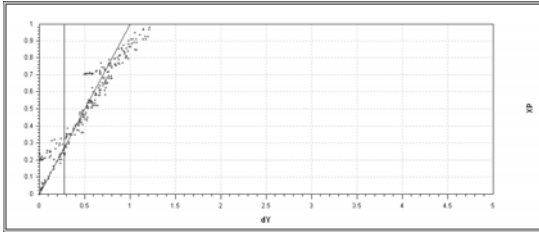


Fig.8 : Diagram $dy-dx$ of the CCA one-dimensional projection of the polarization manifold

This nonlinear bending is even more apparent in Fig.9 which shows the diagram $dy-dx$ for data in the first knee.

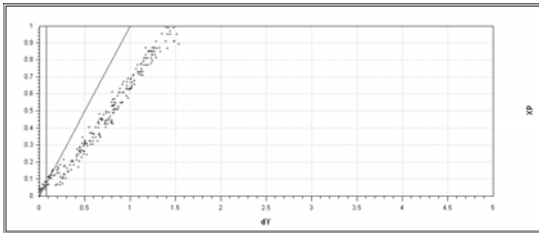


Fig.9: Diagram $dy-dx$ of the CCA one-dimensional projection for the first knee.

An alternative insight into the polarization manifold, justified by its piecewise quasi-linearity, derives from the Principal Component Analysis (PCA), which is a linear projection technique. Fig. 10 shows the 3 first components. The resulting projection is nearly a linear two-dimensional manifold. Physical and analytical considerations suggest that this manifold basically depends on voltage and current and the nonlinearities are mainly limited to these quantities.

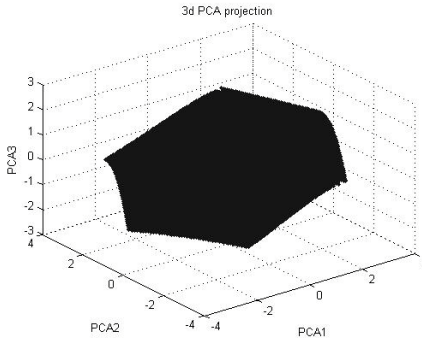


Fig.10: PCA two-dimensional projection of the polarization manifold

5. THE NEURAL CONTROL DESIGN.

This work proposes an indirect neural control design, in which the system is modelled (identified) by a neural approach, but the controller is conventional [10]. The neural approach may consist of an ensemble of neural networks which identify different operating ranges [14]. A gating self-organizing neural network then selects the appropriate neural network (this approach is reminiscent of the P-CMAC network which shows local features [9]). However, considering that the basic nonlinearities depend essentially on current, a simple current look-up table based on currents can replace the gating network. This look-up table identifies the 3 zones (low currents, quasi-linear zone and high currents) and, in a more detail, the two knees. Fig. 11 shows the system identification architecture.

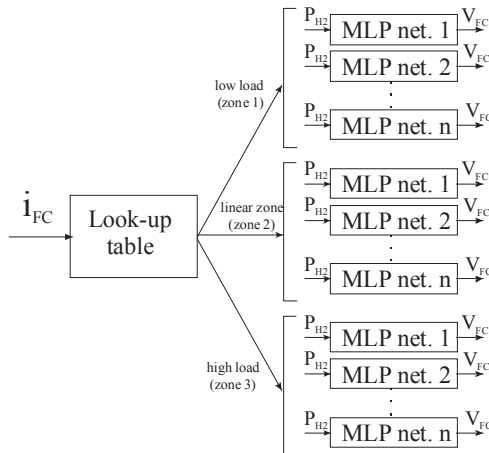


Fig.11: System identification neural ensemble

Each neural network is a Multilayer Perceptron (MLP, [15]), which is a supervised feedforward network. Its adjustable parameters are called weights and are determined from a set of examples (training set, TS) through the process called training. Weights are computed by the prediction error approach, based on the minimization of a measure of closeness in terms of a sum-of-squares error criterion. This minimization is achieved by an iterative search scheme called Levenberg-Marquardt [10], which is a trust-region method based on a second-order approximation of the criterion around the current iterate (Gauss-Newton method). The choice of the inputs (regressor vector) for each neural network is very important. Here a Neural Network AutoRegressive eXternal input (NNARX) model structure has been chosen [10]: the regression vector is composed of the past n inputs and m outputs of the MLP. NNARX is always stable even if the system is unstable, because there is a pure algebraic

relationship between prediction and past measurements and inputs. The lag structure (n and m) for deterministic dynamical systems (under the assumption that the system can be represented accurately by a function that is reasonably smooth in the regressors) can be automatically computed by using a criterion based on the Lipschitz quotients [16], which are computed by using the input-output pairs of the training set for each possible lag space. The resulting index shows a knee for the optimal number of regressors. Fig.12 gives the index plot for the fuel cell system. According to the position of the knee, 2 past inputs and 2 past outputs have been chosen for the NNARX regression vector.

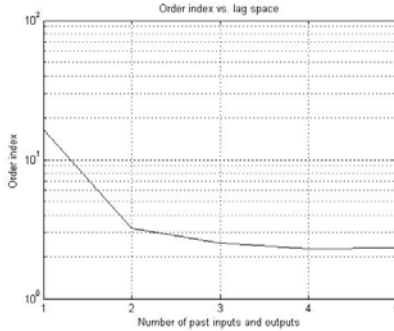


Fig.12 : The index criterion evaluated for different lag spaces (here only $m = n$ is shown)

Here an indirect control design based on the Generalized Predictive Control (GPC, [17], [18]) is proposed. It is a criterion-based approach like the optimal control method (used in a neural approach in [9]), which however can have stability problems and a time-consuming tuning [10]. The predictive controller does not suffer from these drawbacks and is flexible and very powerful. It is based on the minimization of the following criterion:

$$J(t, t) = \sum_{i=N_1}^{N_2} [r(t+i) - \hat{y}(t+i)]^2 + \rho \sum_{i=1}^{N_u} [\Delta u(t+i-1)]^2 \quad (11)$$

with respect to the N_u future control scalar inputs :

$$U(t) = [u(t) \dots u(t + N_u - 1)] \quad (12)$$

and subject to the constraint :

$$\Delta u(t+i) = 0, \quad N_u \leq i \leq N_2 - d. \quad (13)$$

r is the reference signal, d the system delay time, N_1 the minimum prediction horizon (here set equal to d), N_2 the prediction horizon, N_u the control horizon, ρ the weighting factor penalizing changes in the control input (Δ is the difference operator). $\hat{y}(t+k)$ represents the minimum variance k -step ahead

predictor. For the Nonlinear Predictive Control (NPC) the predictor is given by the successive recursion of a deterministic neural network model, as the above cited MLP. The predictor is nonlinear in the future control inputs. The optimization problem must be solved at each sample, resulting in a sequence of future control inputs $U(t)$. From this sequence, the first component $u(t)$ is then applied to the system. The idea of predictive control as applied to the fuel cell is sketched in Fig.13.

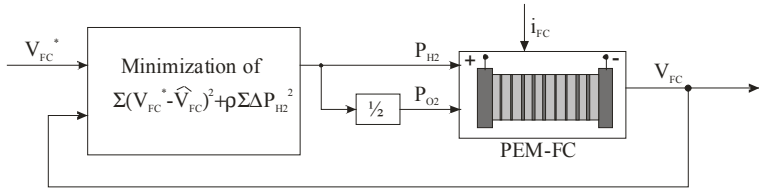


Fig.13 : The predictive control basic idea

Minimization of criterion (11) is a very difficult task and is here achieved by an iterative search procedure. It is based on the Broyden-Fletcher-Goldfarb-Shanno (BFGS, [14]) algorithm which solves the Newton minimization method by producing a positive definite approximation of the inverse of the Hessian of the criterion (11) by employing a consecutive series of previous iterates and corresponding gradients. It is accompanied by a line search for the computation of the step size [14].

The NPC strategy may have several local minima and is computationally demanding. In order to speed up the method, it can be replaced by the Approximate Predictive Control (APC) which applies the instantaneous linearization principle: at each sample a linear model is extracted from a neural network model of the system and a linear controller is designed (see Fig.14). Obviously this can be valid only around the operating point. If a set of operating points is taken into account, a bank of controllers is necessary (gain scheduling [14]).

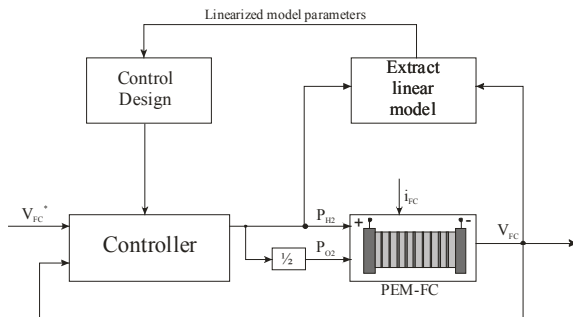


Fig.14 : Control based on instantaneous linearization of a neural predictor

In APC the predictor is given by an approximate minimum variance estimator based on instantaneous linearization of a NNARX model (here an integrated ARX model, ARIX, is achieved). There exists a unique solution of criterion (11) and the future control inputs can be found directly. Hence, it is faster than NPC, but may have a limited validity in certain regimes of the operating range.

6. SIMULATION RESULTS

Both the PEM-FC model and the control system have been simulated in the Matlab-Simulink environment. The training set for the first knee is displayed in Fig.15 and consists of a step function for the input hydrogen partial pressure with increments of 0.5 atm, starting from 0.5 atm up to 10 atm together with the corresponding stack output voltage.. The ascending part has been obtained with a load current of 3 A and the descending one with a load current of 5 A. Similar training sets have been developed for the other zones. In particular the number of the training sets has been chosen high in non-linear zones and small in the linear zone.

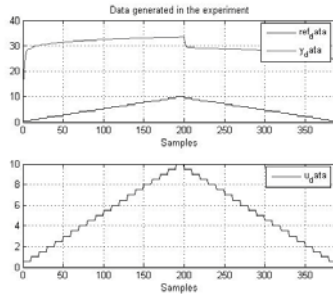


Fig. 15: Training set for the first knee

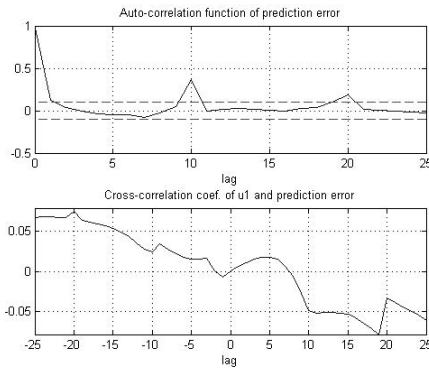


Fig. 16: Correlation tests

For each training set a MLP has been trained for obtaining the forward model. The architecture of the neural network consists of one hidden layer of 9 neurons with hyperbolic tangent as activation function, and one linear output neuron. The regression vector (NNARX), as explained above, is made up of the voltages and pressures of the two previous time samples; the time delay is equal to one time sample.

The training has been accomplished by the Levenberg-Marquardt method. To validate the estimated model a test set has been created and the tests for correlation with different combinations of past residuals (prediction errors) and data have been performed. If the residuals are uncorrelated with all of these combinations, it is likely that all information has been extracted from the training set and that the model approximates the system well. Fig. 16 shows the auto-correlation function of the residual and the cross-correlation between the residuals and the input. It is apparent that the neural network generalises well. Similar analysis has been performed for all the other neural networks.

Fig.17 shows the reference and the actual stack voltage as well as the hydrogen partial pressure with a square wave reference whose average value is 31.5 V and the amplitude is 1.5 V with an initial load current of 1 A and a step load variation up to 5 A after 10 s. The NPC design parameters are: $N_1=d=1$, $N_2=7$, $N_i=2$ and $\rho=0.01$. This figure shows clearly that in this nonlinear area the control system behaves correctly. The output voltage follows the reference predicting the future variations of the reference. At the same time the time variations of the H_2 partial pressure never exceeds the limit value of 10 atm while remaining smooth. In the same working conditions the APC has given bad results, because the instantaneous linearization range is all too little for each operating point in this zone.

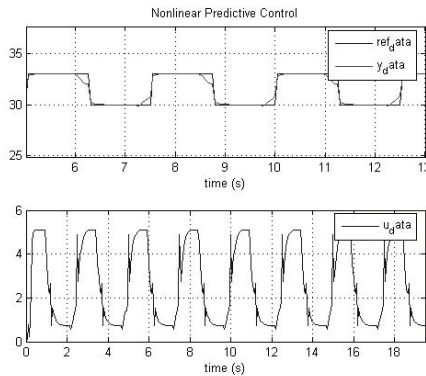


Fig 17: Performance of the NPC in the nonlinear zone.

In the quasi-linear zone (zone of intermediate currents) both the NPC and the APC have been used and compared, as shown in Figs 18-19. In this test a square voltage reference with average value of 26.5 V and amplitude of 1.5 V has been given. The current is maintained constant at 17.5 A. The design parameter of both APC and NPC are the same as before, except for ρ which is now equal to 0.03 in APC and 0.09 in NPC. This choice has been dictated by the consideration that the worse dynamics of APC than that of NPC does not permit a further detuning of the predictor dynamics in favour of a smoother control signal (Fig.18). In the quasi-linear zone the NPS has a better prediction dynamics and a smoother control signal, but on the other hand it is more time consuming because its requires the minimization by BFGS at each sample time.

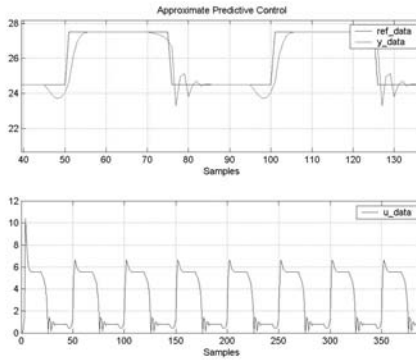


Fig 18: Performance of the APC in the quasi-linear zone

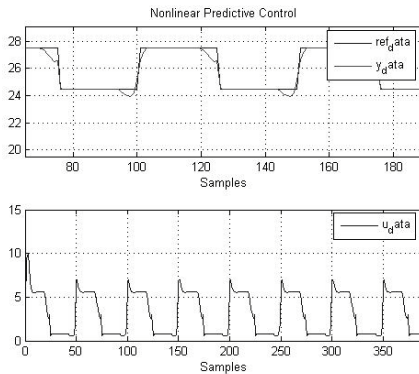


Fig 19: Performance of the NPC in the quasi-linear zone

7. CONCLUSIONS

This paper proposes a neural nonlinear control of PEM-FC by using an existing dynamic model of the fuel cell. The control is a non-linear predictive control whose target is to minimize the variation of the control variable, in this case the hydrogen partial pressure. A series of voltage steps has been given as reference to assess the goodness of the approach in all of the three areas determined by the load current. A suitable look-up table has been used for choosing the proper neural network to be activated for achieving the control action. Numerical results confirm the beneficial effects of the use of this neural control technique, since the input pressure variations are limited. It should be remarked that the use of APC is fully justified only in the quasi-linear zone, while this is not the case in the other areas where the instantaneous linearization is not practically attainable.

ACKNOWLEDGMENTS

Prof. Giansalvo Cirrincione is with the Department of Electrical Engineering University of Picardie-Jules Verne and funded with a grant of ISSIA-CNR, Italy in the framework of the project “Automazione della gestione intelligente della generazione distribuita di energia elettrica da fonti rinnovabili e non inquinanti e della domanda di energia elettrica, anche con riferimento alle compatibilità interne e ambientali, all’affidabilità e alla sicurezza”. This work has been funded by the above project.

8. REFERENCES

- [1] J. M. Corrêa, F. A. Farret, and L. N. Canha, “An analysis of the dynamic performance of proton exchange membrane fuel cells using an electrochemical model,” in *Proc. IEEE IECON’01*, Denver, CO, 2001, pp. 141–146.
- [2] J. M. Corrêa, F. A. Farret, J. R. Gomes, and M. G. Simões, “Simulation of fuel cell stacks using a computer-controlled power rectifier with the purposes of actual high power injection applications,” *IEEE Trans. Ind., Appl.*, no. 4, pp. 1136–1142, Jul./Aug. 2003.
- [3] A. J. Appleby, *Fuel Cell Hand Book*, Van Nostrand Reinhold, New York, 1988.
- [4] J. M. Corrêa, F. A. Farret, L. N. Canha, and Marcelo G. Simões, “An Electrochemical-Based Fuel-Cell Model Suitable for Electrical Engineering Automation Approach”, *IEEE Trans. Ind., Electr.*, VOL. 51, NO. 5, OCTOBER 2004.
- [5] J. T. Pukrushpan, A. G. Stefanopoulou, H. Peng, *Control of Fuel Cell Power Systems*, Springer Verlag, 2004.
- [6] Y. Kim and S. Kim, “An electrical modeling and fuzzy logic control of a fuel cell generation system,” *IEEE Trans. Energy Conversion*, vol. 14, pp. 239–244, June 1999.
- [7] R. F. Mann, J. C. Amphlett, M. A. I. Hooper, H. M. Jensen, B. A. Peppley, and P. R. Roberge, “Development and application of a generalized steady-state electrochemical model for a PEM fuel cell,” *J. Power Sources*, vol. 86, pp. 173–180, 2000.

- [8] J. C. Amphlett, R. F. Mann, B. A. Peppley, P. R. Roberge, and A. Rodrigues, "A model predicting transient responses of proton exchange membrane fuel cells," *J. Power Sources*, vol. 61, pp. 183–188, 1996.
- [9] P. E. M. Almeida and M. G. Simões, "Neural Optimal Control of PEM Fuel Cells With Parametric CMAC Networks", *IEEE Trans. Ind., Appl.*, vol. 41, No. 1, JAN./FEB. 2005.
- [10] M. Norgaard, O. Ravn, N. K. Poulsen, and L. K. Hansen, *Neural Networks for Modeling and Control of Dynamic Systems*. London, U.K.: Springer-Verlag, 2000.
- [11] J. Kim, "Modeling of proton exchange membrane fuel cell performance with an empirical equation," *J. Electrochem. Soc.*, no. 142, pp. 2670–2674, 1995.
- [12] J. E. Larminie and A. Dicks, *Fuel Cell Systems Explained*. Chichester, U.K.: Wiley, 2000, pp. 308–308.
- [13] P. Demartines, J. Héroult, "Curvilinear Component Analysis: a Self-Organizing Neural Network for Non-linear Mapping of Data Sets". *IEEE Trans. Neur. Net.*, vol. 8, n.1, January 1997, pp. 148-154.
- [14] C. M. Bishop, *Neural Networks for Pattern Recognition*, Oxford University Press, 1995.
- [15] S. Haykin, *Neural Networks: A Comprehensive Foundation*, Prentice Hall, 1999.
- [16] X. He, H. Asada, "A New Method for Identifying Orders of Input-Output Models for Nonlinear Dynamical Systems", *Proc. of the American Control Conference*, San Francisco, CA, pp.2520-2523.
- [17] D. W. Clarke, C. Mothadi, P.S. Tuffs, "Generalized Predictive Control-Part I. The Basic Algorithm", *Automatica*, 1987, vol. 23, n. 2, pp.137-148.
- [18] D. W. Clarke, C. Mothadi, P.S. Tuffs, "Generalized Predictive Control-Part II. The Basic Algorithm", *Automatica*, 1987, vol. 23, n. 2, pp.149-160.